COMPLETE STUDY ON DISCRETE TYPES OF GRIDS IN CFD: PREFERRED STRATEGY

K.Swapna
Assistant Professor
Sana Engineering College
Kodada
swapnakandla@gmail.com

ABSTRACT:

The accuracy of the simulation is strongly depends on the quality of the grid. A good quality grid considering the flow physics leads to faster convergence and better solution. This paper deals with nonlinear FVM approach based on different kinds of meshing (using grids-C,O,H).Theory is utilized to obtain the convergence rate, CPU time, coefficient of drag, coefficient of lift, lift/drag of the airfoil (NACA0012). The airfoil considered is studied with three different types of grids viz. O-grid, C-grid and H-grid and accordingly obtain the values of pressure, velocity and temperature. Airfoil is studied with two different flow regimes (i.e., 0.8M & 1.2M). Grid generation is the most critical part of the CFD modeling process and a major part of the computational effort is involved to satisfy certain conditions for valuable CFD results. Good mesh quality, grid alignment to the flow path, proper grid resolution near the boundary zones, etc. are the prerequisites for successful CFD simulation. The choice of finer grid resolution on a certain zone depends on characteristics like the non uniformity in the flow structure, presence of distinct motion type within a flow domain, steep gradient of the flow variables and fluid properties close to the zone, extent of the detail feature required etc. A Finite discretization is applied throughout the process in case of gridding. The computational method does not require any tuning of parameters. The solution obtained shows the good resolution of all flow phenomenon and are obtained by computational analysis. For CFD to be useful in conceptual design, the computational mesh must be built automatically. The generation of structured meshes, made of hexahedral blocks, requires extensive user interaction and skill to create an adequate grid.

Keywords: *Convergence, Airfoil, Descretization, Continuum.*

1.0 INTRODUCTION:

The first one would cover grid generation and the second one we will take up the aspects of validation and verifications, which are essential for any industrial or research CFD analysis. So let us have a look at first lecture in this module, introduction to grid generation. We will basically cover briefly the types of grids, which are there which are normally used in CFD analysis and generation process in brief. And we would briefly discuss about advanced material, which you can refer to, to develop expertise in grid generation. This being an introductory course, we have no intention of introducing the actual numerical techniques which are used in CFD analysis. We will first formally look at what we call a grid that is definition of grid or mesh. Then we would briefly touch upon the classification of grids. Then overall grid generation process, what are the steps involved in grid generation? And then we will look at 2 types of grid generation processes, a structured grid generation and unstructured grid generation. Grid is more common in numerical techniques dealing with finite difference or finite volume applications and mesh is the term, which is most popular in finite element based CFD analysis.

Taking the NACA-0012 airfoil into consideration which has: Maximum

thickness 12% at 30% chord, maximum camber 0% at 0% chord.

NACA-0012

Grid generation of NACA-0012

C-grid: has line of points in one direction roughly like the letter 'C' and one of these line will typically bend back to meet up with itself at some point.
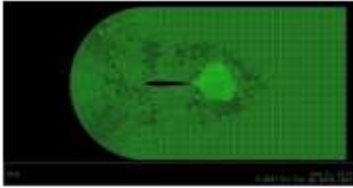

Fig.1. C-grid meshing of an airfoil NACA-0012

The C-mesh generated in fig.1 consists
-40845 quadrilateral cells.
-786 2D Pressure far field faces
-104 2D wall faces
-81245 2D interior faces
-41290 nodes.

O-grid: has lines of points where the last point wraps around and meets the first point, thus you will have some grid lines that look likes letter 'O'.
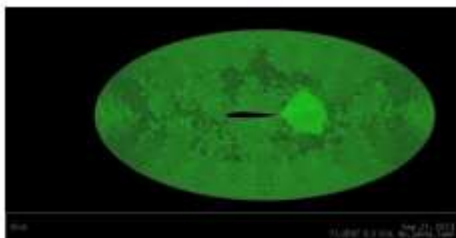

Fig.2. O-grid meshing of an airfoil NACA-0012

The O-mesh generated in fig.2 consists
-37958 quadrilateral cells
-728 2D pressure far field faces
-104 2D wall faces
-75500 2D interior faces
-38374 nodes.

H-grid: is pretty much any structured grid.That is not an c grid and o grid

Fig.3: H-grid meshing of an airfoil NACA-0012.

The H-mesh generated in fig.3 consists
-7203 quadrilateral cells
-360 2D pressure far field faces
-42 2D wall faces
-14205 2D interior faces
-7404 nodes.

Discretization of airfoil by considering a continuum around it for the study of properties such as coefficient of lift, coefficient of drag, convergence rate, CPU time by meshing it with different grids
Analysis of airfoil:
Formulating the airfoil NACA-0012 using Gambit 2.26 and griding it in Ansys-Fluent with c-mesh, o-mesh and h-mesh respectively the following results are obtained.

The research area is restricted to:
Model: Viscous laminar
Boundary circumstances Pressure far turf
Materials: fluids-ideal gas
Pressure velocity coupling simple
Dissertation
Pressure-satndard
Density-first order upwind
Momentum-first order upwind
Energy-first order upwind

2.0 LITERATURE REVIEW:

Sukanta Saha, (2012) Vortical stream structure over sharp edged delta wings are exceptionally mind boggling in nature. The stream field over the upper wing surface is ruled by driving edge vortices. These vortices make suction impact in the region of driving edge inboard which thusly improves the lift power for higher estimations of approach (AoA). The

streamlined qualities of delta wing air ships exclusively rely upon the structure of essential and auxiliary vortices over the wing. In this investigation, surface stream representation strategies are utilized to uncover the topological surface stream structure on a sharp edged 65° delta wing model at subsonic condition. The present examination additionally analyzes the ability of unfaltering state CFD (computational liquid elements) investigation to reproduce the vortical stream field over sharp edged delta wing. Organized matrix structures are produced inside the computational area and Reynolds Averaged Navier Stokes (RANS) based unfaltering state CFD recreations are performed. The trial and computational outcomes are thought about as far as surface stream example and vortex cooperation areas for various AoA.

Karansinghdangi, (2016) In this paper found the drag and lift powers of airplane delta wing utilizing CFD. In exploratory arrangement, the structure model needs to put in testing; this procedure is very troublesome and cost more than CFD strategies cost for the equivalent. In this manner the whole examination experienced computational liquid elements technique .The investigation of the two dimensional subsonic stream over a NACA 64A206 airfoil at different approaches and working at a Reynolds number of 3.57×E+06 is displayed. The CFD reproduction results show great concurrence with hypothetical qualities it prompts suggest a streamlined wing.

Karan Dangi, (2017) The present work portrays by and large audit over the change in streamlined attributes of an airfoil by applying certain surface alterations in type of dimples. Right off the bat, surface adjustments that are considered here are outward and Inward dimples on the wing model. In the wake of picking the better dimpled design as on the after effects of CFD investigation of both, diverse molded dimples are tried and contrasted with the plane airfoil model. This CFD investigation is done in 3-D by taking a section of the airfoil with one dimple on it. A near report demonstrating fluctuation in lift and drag of altered airfoil models at various edge of assaults (AOA) is principle target of this work, [as clarified by Deepanshu in his Paper]. The surface adjustments are done here by thinking about the various kinds and states of dimples. Dimples help in decrease of weight drag when airfoil achieves some approach on the grounds that at same time, wake development introduces because of limit layer division. Utilization of dimples on flying machine wing works in same way as vortex generators would build the by and large streamlined qualities of flying machine, [as clarified by Researchers at Khulna University of Engineering and Technology (KUET), Bangladesh in their Paper]. Use of such outcome into the air ship optimal design upgrades the streamlined attributes and mobility of the air ship. This improvement incorporates the decrease in drag and slow down wonder.

3.0 PROPOSED METHODOLOGY:
Mathematical Models:
The stream around the airfoil has been broke down by unraveling the conditions for preservation of mass and force. Limited volume strategy has been utilized to change over the common conditions of stream in to mathematical conditions that are explained computationally. Weight speed coupling has been finished by SIMPLE calculation. Choppiness of the stream has not been displayed. The

computational subtleties viz. principal conditions that are settled, computationally the subtleties of geometry and geometrical displaying, and matrix age for the wing under examination, outskirts conditions that are authorized are talked about and introduced in this paper. The wind stream around the airfoil is viewed as relentless and compressible.

Governing equations:

The principal navier stokes equations for the flow considered int his work are written in vector form as:

$$\frac{\partial G_1}{\partial x} + \frac{\partial G_2}{\partial y} + \frac{\partial G_3}{\partial Z} = \frac{\partial G_1 y}{\partial x} + \frac{\partial G_2 y}{\partial y} + \frac{\partial 3y}{\partial z}$$

Where G1,G2,G3 are the in viscid flux vector given by:

$$G_1 = \begin{bmatrix} \rho u_1 \\ p + \rho u_1^2 \\ \rho u_1 u_2 \\ \rho u_1 u_3 \end{bmatrix}; \quad G_2 = \begin{bmatrix} \rho u_2 \\ \rho u_2 u_1 \\ P + \rho u_2^2 \\ \rho u_2 u_3 \end{bmatrix}; \quad G_3 = \begin{bmatrix} \rho u_3 \\ \rho u_3 u_1 \\ \rho u_3 u_2 \\ p + \rho u_3^2 \end{bmatrix}$$

G1V, G2V, G3V are the viscous flux velocity, and is given by:

$$G_1 y = \begin{bmatrix} 0 \\ \tau_{xx} \\ \tau_{xy} \\ \tau_{xz} \end{bmatrix}; \quad G_2 y = \begin{bmatrix} 0 \\ \tau_{yx} \\ \tau_{yy} \\ \tau_{yz} \end{bmatrix}; \quad G_3 y = \begin{bmatrix} 0 \\ \tau_{zx} \\ \tau_{zy} \\ \tau_{zz} \end{bmatrix};$$

In the above given equation density is denoted by ρ, the velocities are given by u_1, u_2, u_3 and P is the pressure. Normal stress is given by τ_{xx}, τ_{yy}, τ_{zz} :

$$\tau_{xx} = 2\mu . \frac{\partial u_1}{\partial x} + \mu_{bulk} \left[\frac{\partial u_1}{\partial x} + \frac{\partial u_2}{\partial y} + \frac{\partial u_3}{\partial z} \right]$$

$$\tau_{yy} = 2\mu . \frac{\partial u_2}{\partial y} + \mu_{bulk} \left[\frac{\partial u_1}{\partial x} + \frac{\partial u_2}{\partial y} + \frac{\partial u_3}{\partial z} \right]$$

$$\tau_{zz} = 2\mu . \frac{\partial u_3}{\partial z} + \mu_{bulk} \left[\frac{\partial u_1}{\partial x} + \frac{\partial u_2}{\partial y} + \frac{\partial u_3}{\partial z} \right]$$

The formula for the shape of a NACA 0012 foil, with "12" being replaced by the percentage of thickness to chord, is

$$y_t = \frac{t}{0.2} c \sqrt{\frac{x}{c}} - 0.1260 \left(\frac{x}{c} \right) - 0.3516 \left(\frac{x}{c} \right)^2 + 0.2843 \left(\frac{x}{c} \right)^3 - 0.1015 \left(\frac{x}{c} \right)^4$$

where:

- c - chord length,
- x - position along the chord from 0 to c,
- y - half thickness at a given value of x (centreline to surface), and
- t - maximum thickness as a fraction of the chord (so 100 t gives the last two digits in the NACA 4 - digit denomination).

Note that in this equation, at (x/c) = 1 (the trailing edge of the airfoil), thickness ids negligible and not equal to zero. If zero-thickness trailing edge is considered, for instance for computational effort, any of the coefficients is to be modified such that they sum to zero. Modifying the last coefficient (i.e. to -0.1036) will result in the smallest change to the overall shape of the airfoil.

4.0 RESULTS AND DISCUSSION:

In case of c-grid:

Airfoil NACA-0012 is meshed with C-grid by FVM. Concentration of nodes are higher at leading edge and trailing edge in order to study the flow separation at different flow regimes.

Boundary conditions are applied and flow separations are studied at 0.8M. Leading edge experience high static pressure (approx. 4.21e+04 pascals) and it tends to be negative as it is flowing over the airfoil towards trailing edge. Again there is sudden hike of pressure at trailing edge. Compared to leading edge, pressure is low at trailing edge.
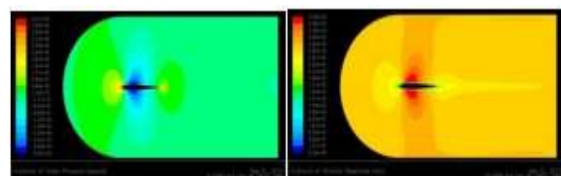
Fig.4. Pressure and Velocity analysis of airfoil in C-grid meshing at 0.8M

Velocity is almost constant at leading edge and trailing edge mainting it at 1.59e+02m/s. There is formation of boundary on airfoil (1.41e+02m/s).

As the flow of velocity is directioned from leading edge to trailing edge velocity reaches it peak point over the surface of airfoil. And ascending on to trailing edge velocity successively subsidies. Continuum conduces static velocity.

From figures 4 and 5:

Table.1 C-Mesh computational analysis results

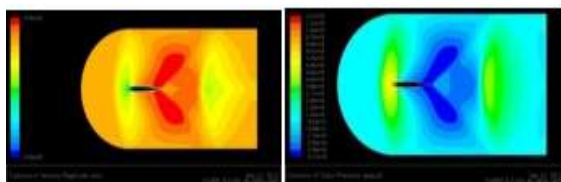|	PRESSURE AT 0.8M	VELOCITY AT 0.8M	PRESSURE AT 1.2M	VELOCITY AT 1.2M
AT L.E	4.21e+04	1.77e+02	1.21e+05	2.53e+01
OVER AIR FOIL	3.04e+04	3.53e+02	-9.33e+02	4.29e+02
AT T.E	2.22e+04	1.59e+02	-3.36e+02	3.54e+02

Fig.5. Pressure and Velocity analysis of airfoil in C-grid meshing at 1.2 M

In case of o-grid:

NACA-0012 is meshed with o-grid by FVM. Concentrations of nodes are higher at leading and trailling edge, to study the parameters varying over it at different flow regimes.
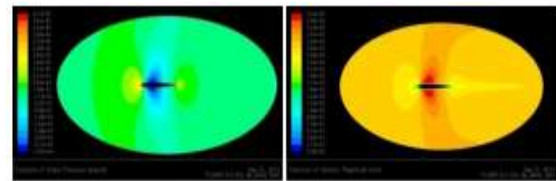

Fig.6. Pressure and Velocity analysis of an airfoil in O-grid meshing at 0.8M

Applying boundary conditions and studying under 0.8M. The pressure on the surface of the airfoil varies from 0-1 co-ordinates. The tip of the leading edge experiences high static pressure(4.17e+04) and vary from LE to TE.

Moving over the surface of airfoil pressure gradually drops out and experiences negativity(-3.07e+04). Moving on to the TE the pressure seems to be constantly moderate(5.50e+04). Velocity parameter seems to be vaying over the outward from TE to LE .The velocity of fluid at the tip of TE is moderate(1.77e+02 m/s). Moving over the surface velocity gradually increases and reaches its peak point at (3.54e+02 m/s) and decreases over the rest of surface. O type grid results are comparitively similar to c type grid.

From figures 6 and 7

Table.2 O-mesh computational analysis results (approx)

	PRESSURE AT 0.8M	VELOCITY AT 0.8M	PRESSURE AT 1.2M	VELOCITY AT 1.2M
AT L.E	3.81e+04	1.77e+02	1.13e+05	7.35e+01
OVER AIR FOI	-3.07e+04	1.77e+02	1.34e+04	3.92e+02

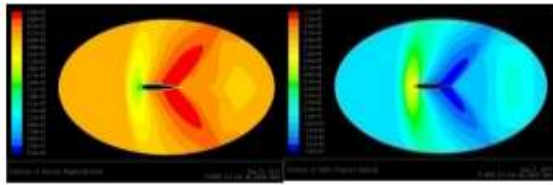| L				
AT T.E	1.27e +04	3.99e +02	- 3.87e +04	3.43 e+0 2

Fig.7. Pressure and Velocity analysis of an airfoil in 0-grid meshing at 1.2M

In case of h-grid

H-grid gives a clear picture of flow separation. Separation of flow over the airfoil, at the tip of leading edge and trailing edge is studied and is analysed. Continum maintains constant air flow. H-grid shows contradict results compared to C-grid and O-grid Static pressure is taken into consideration and pressure in continuum is obtained. Pressure at leading edge is very high compared to that off trailing edge. Static pressure at LE is 3.14e+04 and that of TE is 1.11e+04. Over the surface of airfoil pressure drops out to its negativity. cotinum doesn't show any pressure change it is static at 2.47e+03Pa.
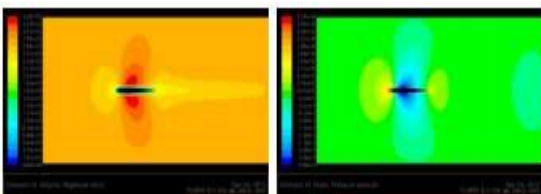

Fig.8. Pressure and Velocity analysis of an airfoil in H-grid meshing at 0.8M

Velocity parameter figures out velocity in continuum. Constant velocity is maintained throughout the continuum at 3.01e+02m/s. Airfoil is bounded by various flow separation layers. On the airfoil velocity is almost negligible, and suddenly its hikes to the highest velocity. At the tip of LE and TE velocity is same (i.e 2.51e+02).

From figures 8 and 9

Table.3 H-mesh computational analysis results (approx)

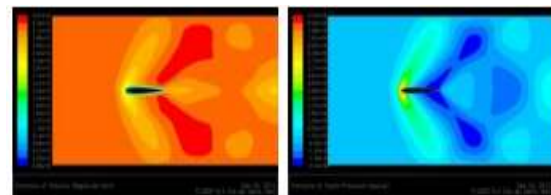|	PRE SSU RE AT 0.8M	VEL OCI TY AT 0.8M	PRE SSU RE AT 1.2M	VEL OCI T Y AT 1.2 M
AT L.E	3.14e +04	6.68e +01	7.42e +04	6.85 e+0 4
OV ER AIR FOI L	- 2.64e +0	3.35e +02	1.24e +04	3.88 e+0 2
AT T.E	- 2.64e +0	3.35e +02	- 1.56e +04	9.14 e+0 1

Fig.9. Pressure and velocity analysis of an airfoil in H-grid meshing at 1.2M
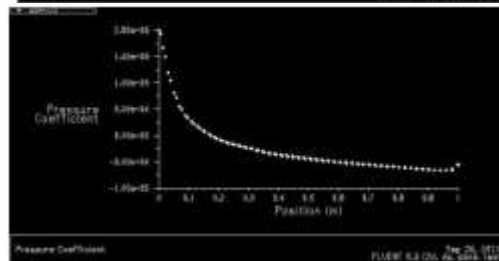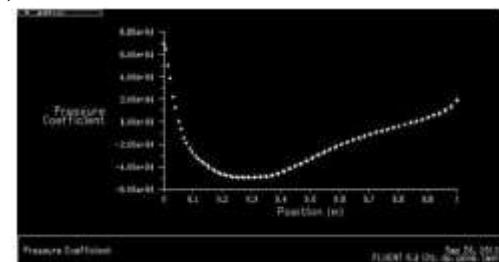**(1)Coefficient of Presuure in C-mesh:**

Fig.10. Coefficient of pressure at 0.8M : Fig.11. Coefficient of pressure at 1.2M

Fig.10 and ,Fig.11 represents the variation of pressure coefficient over NACA-0012 surface at different flow regimes(i.e 0.8M,1.2M) which undegoes the c-grid meshing. Pressure is invariantly fluctuating over LE to TE .At initial stage attack over surface is high, it gradually decreases to the minimum point of the value at the coordinates(0.3 to 0.4).The pressure force later increased suddenly to reach its optimum level at 1.

Airfoil under 1.2M experience its maximum pressure at the prominent edges, considerably decreasing the force of attack over its surface and minimizes it effects on reaching the TE. Bernoulli's principle shows pressure varying inversely such that co-ordinates of velocity changing according to the pressure co-efficient.
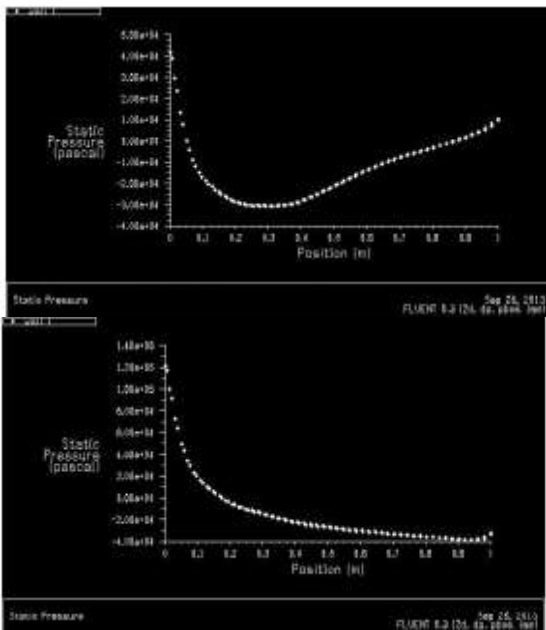
(2)Coefficient of Pressure in O-mesh:

Fig.12.Coefficient of pressure at 0.8M
Fig.13.Coefficient of pressure at 1.2M

As shown in fig.12. pressure is high at the L.E (i.e., 3.81e+04) and dereases over airfoil and again a sudden increase is noticed at the T.E(1.27e+04). In case of 1.2M flow regime pressure decreses from L.E(1.13e+05) to T.E(-3.87e+04) as

represented in fig.13. So at 1.2 M the airfoil experiences low pressure.
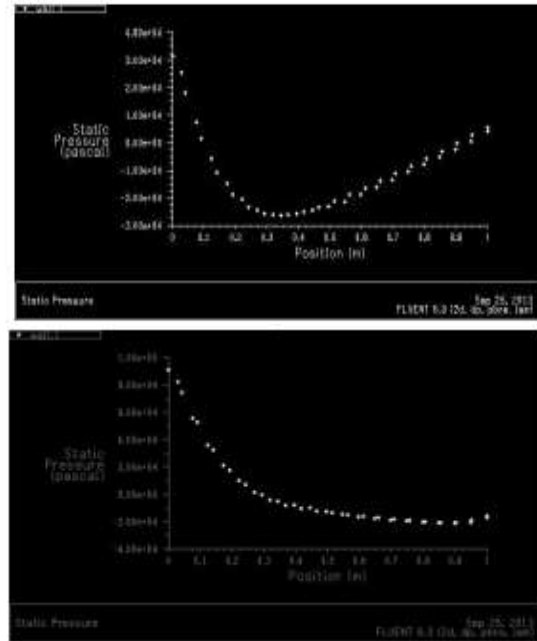
(3)Coefficient of Pressure in H-mesh

Fig.14.Coefficient of pressure at 0.8M
Fig.15.Coefficient of pressure at 1.2M

In fig.14,fig.15, it is observed that ,the variation over h-grid pressure coefficient is fluctuating. Leading limits experiences the high static pressure and reaches to its minimum attack over the region 0.3-0.4 , pressure seems to be increasing gradually over the surface and reaching its ultimate force at the TE. 1.2M flow regime has varying pressure. Attacking over leading edge is very high and exponentially decreases, its minimum attack force reaches to the co ordinate at 1. The variation here is linked with the nodes formed in gridding, since the formed nodes are very low at concentration points the accurate parameters cannot be evaluated.

5.0 CONCLUSION:

It tends to be closed from the above numerical displaying and investigation that the matrix age utilizing C-work and Omesh are sensibly precise when examining the wind stream over an airfoil. It can likewise be inferred that the intermingling of the issue at 1.2M is truly

expending exceptionally high time and memory. Making correlations with writing and different projects, we have precisely had the option to decide the qualities. By directing test work, we can effectively apply similar methods later on to create quality outcomes. Future work will incorporate refining the work to acquire acknowledged estimations of the three coefficients. This will include making the main edge and trailing edge smoother with the goal that stream isn't being upset.

REFERENCES:

1. *A. Milli, S. Shahpar, (2012), PADRAM: Parametric design and rapid meshing system for complex turbomachinery configurations, in: ASME Turbo Expo: Turbine Technical Conference and Exposition, American Society of Mechanical Engineers, 2012, pp. 2135–2148, ASME Paper No. GT 2012-69030.*

2. *H. Blum, (1967), A transformation for extracting new descriptions of shape, Models for the Perception of Speech and Visual Form 362380.*

3. *J.-D. Boissonnat, (2001), Geometric structures for three-dimensional shape representation, ACM Transactions on Graphics (TOG) 3 (4) (1984) 266– 286. [6] N. Amenta, S. Choi, R. Kolluri, The power crust, in: Proceedings of the sixth ACM symposium on Solid modeling and applications, ACM, pp. 249–2*

4. *T. K. Dey, W. Zhao, (2004), Approximating the medial axis from the voronoi diagram with a convergence guarantee, Algorithmica 38 (1) 179– 200.*

5. *Z. Guo, R. W. Hall, (1989), Parallel thinning with two-subiteration algorithms, Communications of the ACM 32 (3) 359–373.*

6. *Y. Zhang, P. Wang, S.-P. Patrick, (1993), Analytical comparison of thinning algorithms, International journal of pattern recognition and artificial intelligence 7 (05) 1227–1246.*

7. *P.-E. Danielsson, (1980), Euclidean distance mapping, Computer Graphics and image processing 14 (3) 227–248.*

8. *H. Xia, P. Tucker, (2010), Finite volume distance field and its application to medial axis transforms, International Journal for Numerical Methods in Engineering 82(1) 114134.*